Neural Network Classification of Mangrove Species from Multi-seasonal Ikonos Imagery

Le Wang, José L. Silván-Cárdenas, and Wayne P. Sousa

Abstract

Tropical forests in many areas of Central and South America experience strong seasonality in climatic variables such as rainfall, solar radiation, wind speed, and relative humidity. Such seasonality is typical of the mangrove forests we study along the Caribbean coast of Panama. Tied to this environmental variation are changes in leaf phenology and physiology that can affect the spectral properties of leaves and thus our ability to discriminate canopies of differing species composition. The goals of this study were two-fold. First, we compared the efficacy of three different classification methods for discriminating mangrove canopies, including a back-propagation, feed-forward neural network classifier with two hidden layers of 24 and 12 neurons (hereafter, BP:24:12*), a newly developed clustering-based neural network classifier (CBNN), and a maximum likelihood classifier (MLC). Comparisons were made with and without added textural information. Our second aim was to compare the absolute and relative discrimination abilities of these methods when applied to images of the same forest acquired in different seasons.*

Two sets of Ikonos images acquired in February (dry season) and May (early wet season) 2004 were analyzed in this study. When only spectral information was considered, MLC and CBNN discriminated differences in canopy species composition with higher accuracy than the BP:24:12 *method. When second-order textural information was also taken into account, CBNN outperformed* MLC *and presented the best classification accuracy, i.e., kappa value equaled 0.93. Analyses of the wet season (May) image were consistently more accurate in discriminating mangrove canopies of differing species composition than analyses of the dry season (February) image, regardless of the classification method or the inclusion of textural information.*

Introduction

Mangrove forests grow along sheltered tropical and subtropical coastlines around the world, and sustain productive, biologically unique, and economically important ecosystems (Lugo and Snedaker, 1974; Tomlinson, 1986; Kathiresan and Bingham, 2001; Alongi, 2002). Over the past 50 years, mangrove habitats have declined dramatically in area due to a variety of anthropogenic disturbances including cutting and filling associated with coastal development and various forms of non-renewable resource exploitation (Ellison and Farnsworth, 1996; Alongi, 2002). Methods for accurately mapping and monitoring changes in the distribution and species composition of mangrove forest canopies will be essential for effective conservation and management of these endangered ecosystems. Since many mangrove forests are difficult to access on foot, due to the flooded, soft sediment environments in which they grow, the development of maps from remotely acquired imagery holds the most promise for monitoring the condition of these forests.

Distinguishing the canopies of different mangrove species with conventional sensors such as Landsat MSS, Landsat TM, and SPOT is difficult due to the low spectral and spatial resolution of such imagery (see Wang *et al.*, 2004a). Such sensors are unsuited to the task of discriminating the relatively small canopies typical of mangrove trees, which in some cases exhibit quite similar spectral signatures. The recent advent of high-resolution, multispectral satellite sensors makes it possible to remotely assess land-cover types at a spatial resolution as great as 61 cm (Wulder *et al.*, 2004). With this enhanced spatial and radiometric resolution, a better classification of individual mangrove species has become possible. However, with this enhanced image resolution comes the challenge of developing analytical approaches that can realize the full potential of the acquired data when attempting to define and discriminate spatial entities. The development of methods for mapping mangrove forests using information collected by high-resolution sensors, particularly at the species-level, is still at an early exploratory stage. Mumby and Edwards (2002) were able to improve thematic accuracy for a marine environment comprised of 13 habitat classes (including mangroves) by incorporating texture information in their analysis of an Ikonos image. Held *et al.* (2003) employed an integrated analysis of data from the high spatial/spectral resolution scanner CASI and the airborne AIRSAR (NASA's polarimetric radar) to map mangrove estuaries along the Daintree River in North Queensland, Australia. Higher classification accuracies of different habitats and mangrove forest types were achieved when hyperspectral and radar data were used in combination, and a slight improvement (around 3 percent) was achieved using a hierarchical neural network in place of MLC. Wang *et al.*(2004a) developed an integrated pixel-based and object-based method, and achieved a moderately accurate result when classifying the canopies of three mangrove species in an Ikonos image. Finally, Wang *et al.*

Le Wang is with the Department of Geography, University at Buffalo, State University of New York, 105 Wilkeson Quad., Buffalo, NY 14261 (lewang@buffalo.edu).

José L. Silván-Cárdenas is with the Department of Geography, Texas State University, San Marcos, TX 78666.

Wayne P. Sousa is with the Department of Integrative Biology, University of California, Berkeley, CA 94720.

Photogrammetric Engineering & Remote Sensing
Vol. 74, No. 7, July 2008, pp. 921–927.

0099-1112/08/7407–0921/$3.00/0
© 2008 American Society for Photogrammetry and Remote Sensing

(2004b) compared the ability to discriminate the canopies of different mangrove species using various combinations of spectral and textural information inherent to Ikonos and QuickBird imagery and concluded that the Ikonos imagery performs slightly better than the QuickBird imagery for this application.

Attempts to classify mangrove species in high spatial resolution satellite images using conventional multivariate classification methods face two major problems. First, what the sensor observes most clearly from the air is the canopy of emergent trees, which may be comprised of different species than the secondary canopy just beneath them, portions of which will also be detected in the interstices between the emergents. Therefore, the spatial distribution of different mangrove species samples in the spectral feature space is often complex. For example, pixels coming from same tree species may reside in several clusters in the feature space. Under such circumstances, an *n*-dimensional (where *n* is the number of features in the feature space) multivariate Gaussian distribution cannot represent the class very well. Second, given the flooded, soft-sediment environment in which mangroves grow, it can be difficult to locate and access pure training and test samples in sufficient numbers for a rigorous MLC-based analysis. Since MLC assumes a Gaussian distribution, a small number of samples can bias the estimation of the variance and covariance matrix.

Our success in developing methods for discriminating mangrove species in high-resolution satellite imagery rests on our ability to overcome these non-trivial biological and logistical constraints. Artificial neural networks (ANN) provide an alternate approach to the statistical approach employed by MLC. ANN provide a more flexible solution to discriminate different classes because no assumption concerning the probability distribution of classes has to be made (Gopal and Woodcock, 1996). The strengths and limitations of neural network applications to remotely sensed imagery are well-covered in the literature (Benediktsson *et al.*, 1990; Paola and Schowengerdt, 1995; Atkinson and Tatnall, 1997). Both variation in the dimensionality of the data set and in characteristics of training and test samples affect the accuracy of learning, as demonstrated by Foody and Arora (1997). Foody (1999) showed that a network trained with samples near the decision boundaries produces lower accuracy of learning but significantly higher accuracy of generalization than one trained with a set of patterns drawn from the cores of the classes. More recently, Liu *et al.* (2003) conducted an experimental study to evaluate the discrimination power of back-propagation feed-forward networks (BPFN) with different degrees of overlap among the classes. They used both simulated and real data for the land-cover classification problem and confirmed that two non-overlapping classes with complex boundaries can be discriminated with 100 percent accuracy with a BPFN; however, discrimination was much poorer with an MLC. Surprisingly, they also found that under conditions of severe overlap, classes with high variability are discriminated better with MLC than with neural networks. They concluded that a hybrid approach might provide the best power of discrimination. One of the major disadvantages of neural networks is the difficulty in obtaining an optimal design, i.e., in determining the minimum number of units in hidden layers that gives the best performance and generalization. Several rules of thumb to properly design a neural network have been proposed in the literature. In particular, the optimal design of a BPFN for land-cover classification were investigated in Kavzoglu and Mather (2003). As an alternative to the back-propagation training strategy, Silván-Cárdenas (2003) proposed the use of unsupervised clustering techniques, coupled with computational geometry methods, as an efficient approach to designing a tree-layered, feed-forward network.

Analysis of remote sensing data collected in different seasons can be useful in maximizing the discrimination power of image interpretation algorithms (Wulder *et al.*, 2004). Seasonal asynchrony in the phenological stages of different vegetation classes or species that results in contrasting spectral signatures can enhance classification accuracy (Dymond *et al.*, 2002). For example, Everitt *et al.* (1996) distinguished Chinese tamarisk, a non-native invasive species, with color infrared aerial photographs acquired during the late fall, which is the phenological stage in which Chinese tamarisk turns a yellow-orange to orange-brown color, contrasting conspicuously with the canopies of other associated plant species. Schriever and Congalton (1995) examined the mapping accuracy of forest cover types in the Northeast with three sets of TM imagery acquired respectively in May (bud-break), September (leaf-on), and October (senescence). Their results indicated that classification was significantly better in October and May than in September owing to differences in chlorophyll absorption rates, water moisture levels, and leaf biomass levels among the seasons.

Our study had the following two objectives: (a) to test the performance of multilayered, feed-forward neural networks for mangrove mapping with Ikonos imagery. Two training strategies were tested: the back-propagation approach and the design-while-training approach proposed in Silván-Cárdenas (2003). The MLC method was also executed to serve as a reference; (b) to determine an optimal season for capturing the spectral difference among mangrove species. Results from this study are expected to contribute to the development of successful methodology for remotely mapping variation in the species composition of mangrove forest canopies.

Methods

Study Site

The study was conducted in mainland mangrove forests near the Smithsonian Tropical Research Institute's Galeta Marine Laboratory (9°24′18″ N, 79°51′48.5″ W) at Punta Galeta on the Caribbean coast of Panama, approximately 8 km northeast of the city of Colon.

Three tree species comprise the canopy of the study forests: black mangrove (*Avicennia germinans*), white mangrove (*Laguncularia racemosa*), and red mangrove (*Rhizophora mangle*). Red mangrove forms a pure or nearly pure stand at the seaward fringe. About 10 to 20 m from the water's edge, white mangrove joins the canopy, forming a nearly even mixture with red mangrove in the low intertidal area. In these mixed-species stands, white mangroves reach average heights of 22 m, while red mangroves average 16 to 18 m in height (W. Sousa, unpublished data). So, the crowns of white mangroves tend to be emergent, and therefore more visible in the satellite image than those of red mangroves, which form a lower sub-canopy. Black mangrove joins the canopy in the mid-intertidal, creating a mixed canopy of the three species, and then gradually monopolizes most upper intertidal stands. White mangrove may disappear completely from the canopy in the upper intertidal, or occur only as scattered individuals or small stands (W. Sousa, unpublished data).

Over the past 31 years, Punta Galeta has received, on average, 2,781 mm of rainfall per year (based on measurements made at the Galeta Marine Laboratory by the Smithsonian Tropical Research Institute's Environmental Science Program). There is marked seasonality in precipitation, with more than 90 percent of rainfall occurring between

early-May and late-December (Cubit *et al.*, 1988 and 1989; Duke *et al.*, 1997). In 2004, the year in which both Ikonos images used in our analysis were acquired, the dry season started on 29 December 2003 and ended on 24 April 2004 (based on criteria developed by the Meteorology and Hydrology Branch of the Panama Canal Authority, Republic of Panama (**http://striweb.si.edu/esp/physical_monitoring/summary_seasons.htm**). During the 30 days prior to 02 February 2004 (the date of the dry season image), 34 mm of rain fell at Galeta, as compared to 257 mm of rain that fell during the 30 days prior to 08 May 2004 (the date of the early wet season image). Aspects of mangrove phenology exhibit a strong association with seasonal rainfall patterns. We regularly observe that new leaves are flushed primarily during the wet season, and this pattern was quantified for *Rhizophora mangle* on Punta Galeta by Duke and Pinzón (1993). They found that leaf production was lowest from December to February (dry season) and peaked in May to July (early wet season). Since the spectral properties of leaves change as they age (Carter *et al.*, 1989), we would expect canopy reflectance to change seasonally with the shift in average leaf age. In addition, as a consequence of lower rainfall and higher evaporation, soil salinities are substantially higher during the dry season (W. Sousa, unpublished data); this combination of drought conditions and high soil salinity is likely to lead to reduced leaf water content and enhance water stress, thereby affecting leaf reflectance (Carter, 1991 and 1993).

Data Collection and Preprocessing

Two scenes of Ikonos Geo-Bundle images were employed in this study. They were acquired on 02 February 2004 at 1604 local time and 08 May 2004 at 1601 local time. Metadata for the two sets of images indicate that both were collected at a similar sensor elevation: 85.8° for the February images and 79.1° for the May images. The high elevation angle largely offsets the geometric distortion induced by variation in terrain elevation, which is very modest in mangrove habitats. An image to image registration was conducted using May imagery as the reference image and a registration error; a root mean square (RMS) of 0.5 pixels was reported. A nearest neighbor resampling approach was adopted to rectify the February image.

Back-Propagation Neural Networks Classifier (BPNN)

A BPNN is a multi-layered feed-forward network trained by the so-called back-propagation algorithm as first introduced by Rumelhart *et al.* (1986). This learning algorithm, also called the generalized delta rule, is an iterative gradient descent training procedure. It is carried out in two stages. In the first stage, once the network weights have been randomly initialized, the input data are presented to the network and propagated forward to estimate the output value for each training pattern set. In the second stage, the difference (error) between known and estimated outputs is minimized. The whole process is repeated, with weights being recalculated at every iteration, until the error is minimal, or lower than a given threshold. For the classification problem a BPNN classifier recognizes spectral patterns by learning from training sets. After training, the neural network system fixes all the weights and maintains the original learning parameters. The classification process calculates the output of each pixel using the parameters learned from the training phase, and then decides the class assignment of the pixel.

In this study, a BPNN with two hidden layers of 24 and 12 neurons, respectively, hereafter referred to as BP:24:12, was trained using the MATLAB Neural Network Toolbox (V4.0.2-R13). One input node per band and one output neuron per class were employed with the output encoding convention of a high level (0.9) from the output neuron corresponding to a given class and simultaneously low output (0.1) from other output neurons. Each neuron computes a log-sigmoid function of the weighted sum of its input. The updates of the weights and activation level parameters were carried out using the Levenberg-Marquardt optimization method for 100 epochs.

Clustering-based Neural Network Classifier (CBNN)

The second method we evaluated was introduced by Silván-Cárdenas (2003). This method is carried out in two stages. In the first stage, the ISODATA algorithm is run on each training set to identify a number of clusters for each class. Each cluster center is labeled according to the class to which it belongs, and the entire set is used to build a Delaunay graph. In the second stage, a three-layered, feed-forward network is built as follows. For each pair of nodes belonging to different classes that are connected in the Delaunay graph, a neuron is created in the first hidden layer and its weight parameters are set to the coefficients of the hyperplane that separates the two clusters in question. A second layer of neurons is then added to perform the intersection of the half-spaces defined by the first layer to form the largest convex regions, each of which falls into a single class. Finally, the output layer joins the convex region into arbitrarily complex non-convex regions which define the decision region for each class.

It must be noted that the activation functions for all units are implicitly considered as hard limiters (or step functions) during the design stage. However, log-sigmoid functions may be used in the classification process. In the latter case a smoothing parameter is considered and the hard limiter results as a limiting process. More specifically, the sigmoid function is defined by:

$$f(s) = \frac{1}{1 + e^{-s/\alpha}}$$

where α is the smoothing parameter. As α approaches to zero, the plot of $f(s)$ tends to a hard limiter function.

The effect of the smoothing factor on the classification boundaries is illustrated in Figure 1. The small patches apparent in Figure 1a are mainly due to the overlap among black mangrove, red mangrove and rain forest classes. After introducing the smoothing factor, the decision boundaries turn smoother, and consequently, small patches may disappear (Figure 1b). Since different smoothing factors lead to different classification accuracies, a natural question to ask is how we can choose the best value for the smoothing parameter. In previous work, Silvan-Cárdenas (2003), α was empirically set to 0.02. In this study, we developed a scheme to choose the optimal parameter α with which the kappa value is at a maximum. The plot of the kappa value against α obtained for the data set of May is shown in Figure 2. In this case, the optimum smoothing factor falls around 0.01. After several trials, it was observed that the optimum α most likely lies at 0.015, which confirms that 0.02 is a good empirical choice. Another interesting observation is the fact that the optimum α based on the testing set (and still using the same trained network) reports a similar value as the optimum α based on the training set. This might indicate that (a) the training sample is representative of the classes under consideration, and (b) the network can generalize very well the data that are not previously included in the training samples. Evidently, the second conclusion can be a consequence of the first one only if the training method succeeds.

This method was implemented in MATLAB software. The classifier is hereafter referred to as CBNN.

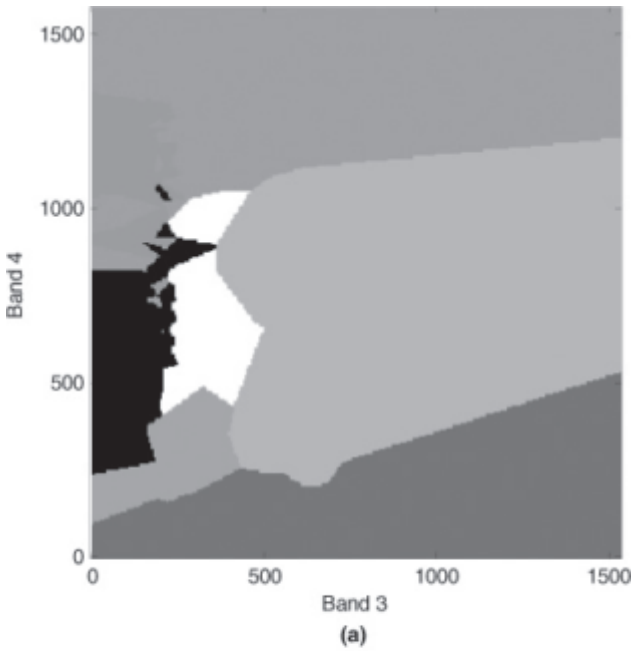

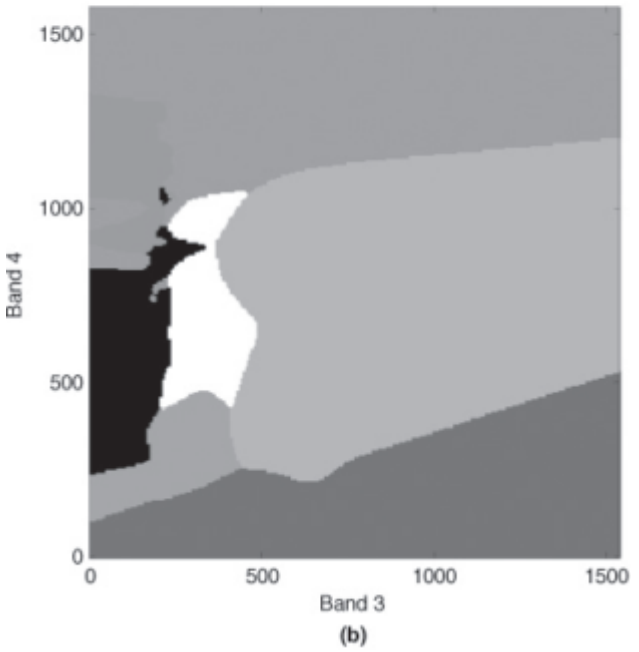

Figure 1. Decision region defined by the CBNN with (a) hard limiter functions, and (b) sigmoid functions with $\alpha = 0.01$. Only band 3 and band 4 from the May 2004 data where used as input in this example. A color version of this figure is available at the ASPRS website: **www.asprs.org**.

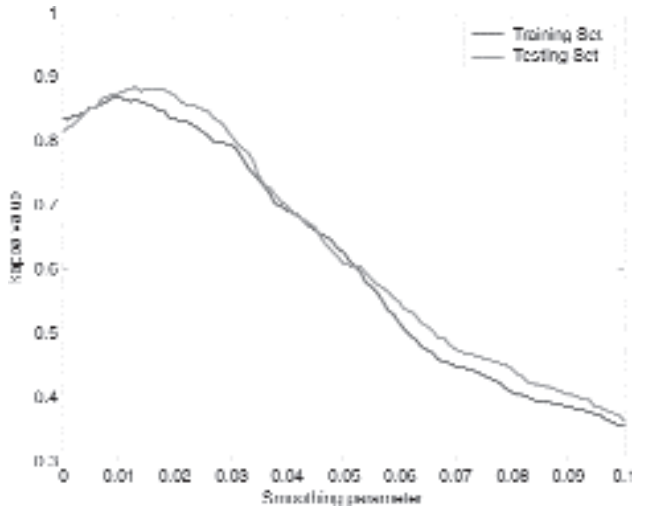

Figure 2. Plot of kappa value against the smoothing factor. Optimum smoothing parameter is 0.01. A color version of this figure is available at the ASPRS website: **www.asprs.org**.

Maximum Likelihood Classifier (MLC)

Previous research has indicated that the maximum likelihood classification is the most effective method for distinguishing mangrove from non-mangrove habitat using data from traditional satellite sensors (Gao, 1998 and 1999; Green *et al.*,1998; Held *et al.*, 2003). However, there are a number of open questions concerning the usefulness of MLC for classifying the species composition of mangrove forests in high-resolution images, which capture the considerable small-scale spatial heterogeneity typical of mangrove canopies. The decision rule of MLC is defined by the multi-dimensional normal distribution around a class mean. Consequently, multi-modal or non-normally distributed data will lead to an incorrect classification. In addition, overlapping decision boundaries in feature space are problematic, especially if the training data do not physically overlap, but the decision boundaries do overlap. In our study, we have used MLC as a reference method for assessing neural network performance. Equal *a priori* probability was assumed for all the classes in the implementation of MLC.

Results

To compare classification performance of the two images, spatially consistent training and test samples were prepared with the aid of two field surveys carried out in January and July 2004, close to the times of image acquisition. During both field surveys, an extensive number of GPS points were measured by a high-precision Trimble GPS (Pathfinder® Pro XRS receiver). The species type, percentage of surrounding vegetation, as well as other tree inventory information, such as DBH and crown area, were recorded as well. Given the patchy distribution of mangrove species, we used polygon tools to define training and test samples on the images. In reference to the field collected GPS points, small polygons, each encompassing no more than 10 pixels, were delineated across the study area to serve as training and test samples. Special caution was made to only choose polygons that fall in pure stands of a specific species in order to avoid including mixed pixels. The total number of samples was reported in Table 1. Two experiments were designed to assess the accuracy of each classification method given two different combinations of input bands: spectral bands only, or spectral and textural bands. The results were reported in detail as follows.

Classification Based on Spectral Information

In the first experiment, the four multispectral bands were employed as input bands while the panchromatic band was not taken into account. For each classifier the overall kappa value was computed using both the training and test sample

TABLE 1. TRAINING AND TEST SAMPLE SIZES

Sample Types	Red mangrove	Black mangrove	White mangrove	Gap	Lagoon	Rainforest	Road
Training	299	220	167	71	155	338	55
Test	205	185	108	82	58	115	51

sets to analyze its generalization characteristic. Intuitively, one should expect lower kappa values for the test set than for the training set. A kappa value based on the training set represents the ability of the model to fit the training data, however a kappa based on the test set reveals the capability of the model to generalize (i.e., achieve the correct classification of data not previously encountered). Therefore, the ratio of the later with respect to the former is an index of the level of generalization achieved by a supervised classifier, provided that the number of samples in both sets is sufficiently large for rigorous statistical comparison. The corresponding kappa values and generalization ratio for the tested classifiers are shown in Table 2. Three results are clearly discernable. First, in general the CBNN and MLC classifiers performed better with the May image than with the February image, while the BP:24:12 classifier displayed lower accuracy with the May than February image. Second, the CBNN and MLC classifier considerately outperformed the BP:24:12 for the May image in terms of both the kappa value and the generalization ratio. The three classifiers achieved comparable accuracy when applied to the February image. Third, MLC yielded the highest generalization ratios (0.99 and 1.05) for both images.

User accuracy was derived for each classifier and land cover type (Table 2). For the individual mangrove species, user accuracy ranged from 35.6 percent (for black mangrove in the May image with the BP:24:12 classifier) to 96 percent (for white mangrove in the May image with the CBNN classifier). The CBNN and MLC classifiers were noticeably more accurate than BP:24:12 when applied to either image, while in general, MLC gave consistently high user accuracy for the three mangroves in both images.

Classification Based on Textural and Spectral Information

As detailed above, the CBNN and MLC classifiers provided reasonably high overall classification accuracy when only spectral bands were considered. Given the high spatial detail associated with the panchromatic band of the Ikonos image, it was of interest to further investigate how well these two classifiers can utilize added textural information in assisting the classification process. In this experiment, the second order texture method, Grey Level Co-occurrence Matrix (GLCM), was adopted to extract the textural information from the panchromatic band of the Ikonos image. Displacement vectors at four directions (0, 45, 90, and 135 degrees), with a spatial distance of one pixel, were employed to compute three rotation invariant texture bands: Contrast (CON), Entropy (ENT), and Angular Second Moment (ASM) at three different window sizes: 9*9, 17*17, 25*25, respectively. The quantization level was set to 16 in all cases. Then, each texture band was resampled to the same resolution as the multispectral bands (4 m), and stacked together with the four multispectral bands as the input bands for the CBNN and MLC classifier. For the CBNN method, the smoothing parameter was fixed to 0.015, which is consistent with what was described in the CBNN section. The respective kappa values based on the test samples are presented in Table 3.

The addition of textural bands to the multispectral bands significantly improved the classification results for both CBNN and MLC (Table 3). For the February image, the kappa values increased to 0.88 for CBNN and 0.8 for MLC, compared to 0.78 and 0.79, respectively, when only multispectral bands are included. Likewise, for the May image, the kappa values when textural information was included were 0.93 for CBNN and 0.89 for MLC, compared to 0.87 and 0.83, respectively, when textural information was not included. Furthermore, when textural information was included, analyses of the May image yielded consistently superior classification at all window sizes when compared to analyses of the February image. Finally, textural information extracted from a larger window size was more instructive than that from a smaller window size.

Discussion and Conclusion

Multitemporal information can be very helpful in discriminating the canopies of different forest species (Jensen 2004). Our results confirmed that multi-seasonal imagery can aid species-level classification of mangrove forests. Our study found that an Ikonos image acquired during the early rainy season more effectively captured the difference among mangrove species than one taken during the dry season. This difference is probably attributable to phenological and physiological changes that affect the reflectance of tree

TABLE 2. ACCURACY OF THE THREE CLASSIFICATION METHODS FOR THE FEBRUARY AND MAY IKONOS IMAGES USING MULTISPECTRAL BANDS ALONE

	04 February			04 May		
Land-cover category	BP:24:12	CBNN	MLC	BP:24:12	CBNN	MLC
Red mangrove	88.8	81.6	86.6	44.3	94.3	92.6
White mangrove	56.8	65.6	73.3	82.1	96.0	92.4
Black mangrove	68.2	64.4	72.5	35.6	78.8	91.5
Gap	93.7	85.9	82.2	0.0	96.2	89.3
Lagoon	100.0	100.0	100.0	83.7	90.6	90.0
Rainforest	72.7	73.8	78.4	91.7	89.1	84.3
Road	94.6	100.0	89.9	90.4	98.0	71.8
Kappa (test samples)	**0.74**	**0.73**	**0.78**	**0.49**	**0.87**	**0.86**
Kappa (training samples)	**0.79**	**0.78**	**0.79**	**0.6**	**0.87**	**0.83**
Ratio	**0.94**	**0.94**	**0.99**	**0.83**	**1.00**	**1.05**

TABLE 3. KAPPA VALUES FOR THE CBNN AND MLC ANALYSES OF FEBRUARY AND MAY IMAGES USING BOTH MULTISPECTRAL AND TEXTURAL BANDS

	February Ikonos		May Ikonos	
Window Size	CBNN	MLC	CBNN	MLC
9	0.86	0.77	0.91	0.85
17	0.88	0.79	0.92	0.87
25	0.87	0.80	0.93	0.88

canopies. At our study sites, mangroves flush new leaves during the early wet season, while they experience stress from drought and high soil salinity during the dry season.

When only multispectral bands were included in the classification, MLC proved the best method for discriminating different mangrove species, consistent with the findings of other studies, mentioned above. CBNN demonstrated a similar performance but at the cost of a considerable increment in computing time. However, when textual information was added to the classification, CBNN exhibited a strong advantage over MLC in characterizing the complex decision boundary associated with the combination of textural and spectral bands. The relative loss in MLC's power of discrimination when textural information was incorporated could have resulted from a violation of its central assumption of a multivariate Gaussian distribution model, as discussed earlier. Neural network-based analyses do not rest on this assumption, and thus gained discrimination power from the added textural information. Compared to the traditional back-propagation neural network method, the new CBNN method provides a computational simpler yet effective way in discriminating different mangrove species.

Acknowledgments

This study was supported by grants to Le Wang from the National Science Foundation (DEB-0810933), W.P. Sousa from the National Science Foundation (DEB-0108146), and the U.C. Berkeley Committee for Research. The second author thanks CentroGeo, Mexico for the support provided while studying at Texas State.

References

Alongi, D.M., 2002. Present state and future of the world's mangrove forests, *Environmental Conservation*, 29:331–349.

Atkinson, P.M., and A.R.L. Tatnall, 1997. Neural networks in remote sensing – Introduction, *International Journal of Remote Sensing*, 4:699–709.

Benediktsson, J.A., P.H. Swain, and O.K. Ersoy, 1990. Neural network approaches versus statistical-methods in classification of multisource remote-sensing data, *IEEE Transactions on Geoscience and Remote Sensing*, 4:540–552.

Carter, G.A., K. Paliwal, U. Pathre, T.H. Green, R.J. Mitchell, and D.H. Gjerstad, 1989. Effect of competition and leaf age on visible and infrared reflectance in pine foliage, *Plant Cell and Environment*, 12:309–315.

Carter, G.A., 1991. Primary and secondary effects of water content on spectral reflectance of leaves, *American Journal of Botany*, 78:916–924.

Carter, G.A., 1993. Response of leaf spectral reflectance to plant stress, *American Journal of Botany*, 80:239–243.

Cubit, J.D., R.C. Thompson, H.M. Caffey, and. D.M. Windsor, 1988. Hydrographic and meteorological studies of a Caribbean fringing reef at Punta Galeta, Panama: Hourly and daily variations for 1977–1985, *Smithsonian Contributions in Marine Science*, 32:1–220.

Cubit, J.D., H.M. Caffey, R.C. Thompson, and D.M. Windsor, 1989. Meteorology and hydrography of a shoaling reef flat on the Caribbean coast of Panama, *Coral Reefs*, 8:59–66.

Duke, N.C., and M.Z.S. Pinzón, 1993. Mangrove forests, *Long-term Assessment of the Oil Spill at Bahía Las Minas, Panama, Synthesis Report, Volume II: Technical Report* (B.D. Keller and J.B.C. Jackson, editors), OCS Study MMS 93–0048, U.S. Department of the Interior, Minerals Management Service, Gulf of Mexico OCS Region, New Orleans, Louisiana, pp. 447–533.

Duke, N.C., M.Z.S. Pinzón, and M.C. Prada, 1997. Large-scale damage to mangrove forests following two large oil spills in Panama, *Biotropica*, 29:2–14.

Dymond, C.C., D.J. Mladenoff, and V.C. Radeloff, 2002. Phenological differences in tasseled cap indices improve deciduous forest classification, *Remote Sensing of Environment*, 3:460–472.

Ellison, A.M., and E.J. Farnsworth, 1996. Anthropogenic disturbance of Caribbean mangrove ecosystems: Past impacts, present trends, and future predictions, *Biotropica*, 4:549–565.

Everitt, J.H., D.E. Escobar, M.A. Alaniz, M.R. Davis, and J.V. Richerson, 1996. Using spatial information technologies to map Chinese tamarisk (*Tamarix chinensis*) infestations, *Weed Science*, 1:194–201.

Foody, G.M., 1999. The significance of border training patterns in classification by a feedforward neural network using back propagation learning, *International Journal of Remote Sensing*, 18:3549–3562.

Foody, G.M., and M.K. Arora, 1997. An evaluation of some factors affecting the accuracy of classification by an artificial neural network, *International Journal of Remote Sensing*, 4:799–810.

Gao, J., 1998. A hybrid method toward accurate mapping of mangroves in a marginal habitat from spot multispectral data, *International Journal of Remote Sensing*, 10:1887–1899.

Gao, J., 1999. A comparative study on spatial and spectral resolutions of satellite data in mapping mangrove forests, *International Journal of Remote Sensing*, 14:2823–2833.

Gopal, S., and C. Woodcock, 1996. Remote sensing of forest change using artificial neural networks, *IEEE Transactions on Geoscience and Remote Sensing*, 34:398–404.

Green, E.P., C.D. Clark, P.J. Mumby, A.J. Edwards, and A.C. Ellis, 1998. Remote sensing techniques for mangrove mapping, *International Journal of Remote Sensing*, 5:935–956.

Held, A., C. Ticehurst, L. Lymburner, and N. Williams, 2003. High resolution mapping of tropical mangrove ecosystems using hyperspectral and radar remote sensing, *International Journal of Remote Sensing*, 24:2739–2759.

Jensen, J.R., 2004. *Introductory Digital Image Processing: A Remote Sensing Perspective*, Third edition, Upper Saddle River, New Jersey, Prentice Hall, 526 p.

Kathiresan, K., and B.L. Bingham, 2001. Biology of mangroves and mangrove ecosystems, *Advances in Marine Biology*, 40:81–251.

Kavzoglu, T., and P.M. Mather, 2003. The use of backpropagating artificial neural networks in land cover classification, *International Journal of Remote Sensing*, 23:4907–4938.

Liu, X.H., A.K. Skidmore, and H. Van Oosten, 2003. An experimental study on spectral discrimination capability of a backpropagation neural network classifier, *International Journal of Remote Sensing*, 4:673–688.

Lugo, A.E., and S.C. Snedaker, 1974. The ecology of mangroves, *Annual Review of Ecology and Systematics*, 5:39–64.

Paola, J.D., and R.A. Schowengerdt, 1995. A review and analysis of backpropagation neural networks for classification of remotely-sensed multispectral imagery, *International Journal of Remote Sensing*, 16:3033–3058.

Rumelhart, D.E., G.E. Hinton, and R.J. Williams, 1986. Learning representations by back-propagating errors, *Nature*, 323:533–536.

Schriever, J.R., and R.G. Congalton, 1995. Evaluating seasonal variability as an aid to cover-type mapping from Landsat Thematic Mapper data in the northeast, *Photogrammetric Engineering & Remote Sensing*, 61(3)321–327.